PERFORMANCE EVALUATION OF A SUSTAINABLE AND ENERGY EFFICIENT RE-ROOFING TECHNOLOGY USING FIELD-TEST DATA

Kaushik Biswas, William Miller and Phillip Childs
Oak Ridge National Laboratory
Oak Ridge, Tenn., U.S.

Jan Kośny
Fraunhofer Center for Sustainable Energy
Cambridge, Mass., U.S.

Scott Kriner
Metal Construction Association
Glenview, Ill., U.S.

Keywords

Phase change material, thin-film photovoltaics, roof retrofit, metal roofs.

Abstract

During September-October 2009, a research team of members representing Metal Construction Association, a North American trade association of metal building manufacturers, builders, and material suppliers; CertainTeed, manufacturer of thermal insulation and building envelope materials; Uni-Solar, producer of amorphous silicon photovoltaic (PV) laminates; Phase Change Energy Solutions, manufacturer of bio-based phase change material (PCM); and Oak Ridge National Laboratory (ORNL) installed an experimental retrofit roof in the ORNL campus. The objective was to evaluate a new sustainable re-roofing technology utilizing amorphous silicon PV laminates integrated with metal roof panels and PCM heat sink. The experimental attic with PV laminate is expected to work during winter as a passive solar collector with the PCM storing solar heat absorbed during the day, and increasing overall attic air

temperature at night. During summer, the PCM is expected to act as a heat sink at the roof, reducing the heat gained by the attic and consequently, lowering the cooling-load on the building.

Field-test data of the experimental PV-PCM attic are presented and discussed. Performance of the PV-PCM attic is evaluated by comparing it to a control attic with an asphalt shingle roof. The test results showed that substantial energy and cost savings are possible with the current experimental roof. Solar power generation data from the PV laminates installed over the PCM attic are also presented.

Authors

Kaushik Biswas**:** Dr. Biswas is a R&D Associate within the Building Envelopes Research Group at Oak Ridge National Laboratory. His research is focussed on whole building energy performance analysis, which includes evaluation of roofs, attics, walls and foundations for their impacts on building energy efficiency. He's also involved in research related to ignition and flammability characteristics of building exteriors. Currently, he is working on updating an attic simulation model described in ASTM C 1340 (2004), to a newer Fortran version. His other research activities include thermal transmission property measurements of building materials and wall assemblies, building thermal integrity assessment using infrared thermography and evaluation of building integrated photovoltaic modules. Dr. Biswas completed his M.S. and Ph.D. from Purdue University with specialization in combustion and flame radiation analysis. His Bachelor of Engineering is from Rajiv Gandhi Technological University in India. His other industrial experience is in investigation of building and vehicle fires for cause and

origin determination. He is a participating member of ASTM committee C16 & a full member of the honor society Sigma-Xi.

William (Bill) Miller: Dr. Miller is a specialist with 32 years of experience in building science, absorption heat and mass transfer and vapor compression refrigeration systems. He has a Ph.D. in Mechanical Engineering, and works for the Energy and Transportation Sciences Division of the Oak Ridge National Laboratory.

Phillip Childs: Phil Childs is responsible for thermal performance testing of wall systems in the Rotatable Guarded Hot Box (RGHB) and for the testing of material properties in the hygrothermal test lab. His qualifications include: expertise in the design and implementation of sensors and data acquisition systems for monitoring in-house and field experiments; proficiency in building envelope diagnostics through the use of blower doors and infrared thermal imaging systems; and experience assessing the durability and energy efficiency of field-installed reflective roofing membranes. Phil is a Research Associate at Oak Ridge National Laboratory, with 35 years of experience. His education includes a B.S., Organizational Management - Tusculum College and Associate of Science, Pre-engineering - Roane State Community College.

Jan Kosny: Dr. Jan Kosny is a civil engineer with almost 30-years of experience in building science, building solar applications, thermal testing of building envelope materials and systems, and energy analysis. He specializes in experimental and theoretical analysis of energy performance of building envelope materials and systems, thermal storage, and building integrated solar technologies. He received his Ph.D. in Building Physics from the Institute of Fundamental Technological Research, Polish Academy of Sciences, Warsaw, Poland. Dr. Kosny had been a member of the ORNL

research staff since 1992. He previously worked as an assistant professor at the Civil and Architectural Engineering Department Technical University of Rzeszow, Poland. Since 2005, he is also an Adjunct Professor in the School of Graduate Studies in Forestry and Environmental Management, University of New Brunswick, Canada. Since July 2010, Dr. Kosny leads building enclosure research at the Fraunhofer-MIT Center for Sustainable Energy Systems. He is a member of ASHRAE TC 04.04 on Building Materials and Building Envelope Performance, TC 02.08 on Building Environmental Impacts and Sustainability, TC 04.07 on Energy Calculations, and ASTM C-16 Committee on thermal Insulation. Dr. Kosny is a Member of the Editorial Board of the Journal of Building Physics and the Nordic Journal of Building Physics. Since 2009, Dr. Kosny represents the U.S. in the IEA-SHC Task 42 / Annex 24 - Compact Thermal Energy Storage.

Scott Kriner: Scott Kriner is President of Green Metal Consulting, Inc. and serves as the technical director of the Metal Construction Association. He is also consulting for manufacturers and suppliers of metal roofing and wall systems. He is a contributing author to many trade publications and serves on the Advisory Board of the Eco-Intel project. He is a LEED Accredited Professional and a published author of a book titled “Wait and See”. Prior to establishing his consulting firm, Scott was Technical Marketing Manager-Building Products for Akzo-Nobel Coatings, Inc. He started his career in 1981 with Bethlehem Steel in the coated steel research department at Homer Laboratories. Scott has experience in the domestic and international metal and coatings industry and has held numerous positions of responsibility in industry and trade organizations. He is the founding chairman of the Cool Metal Roofing Coalition which was formed in 2002,

and serves as Vice Chair of the Cool Roof Rating Council's Technical Committee. Scott serves on the Advocacy Committee of the Lehigh Valley Branch of the Delaware Valley Green Building Council, is a member of the ASTM Committee E60 on Sustainability, and is a board member of the Roofing Industry Committee on Weathering Issues (RICOWI). Scott has B.S. and Masters degrees in Metallurgy and Materials Engineering from Lehigh University in Bethlehem, PA. He holds a patent of improvement on 55 percent Al-Zn Alloy Coated Steel.

Introduction

According to the National Association of Home Builders (NAHB), asphalt shingle is the most commonly used roofing material in new home construction and reroofing, accounting for over 60 percent of the residential roofing market in the U.S. Asphalt roofs generally carry 10-50 year and lifetime warranties, and require replacement or recovery at the end of their service lives. In the U.S., reroofing generates an estimated 6.8 million tons of waste asphalt shingles each year. One of the biggest environmental drawbacks of re-shingling a roof is disposal of the old materials. The old shingles require large disposal areas and pollute the environment over time [1, 2]. To reduce landfill, the recycling of waste asphalt shingles has gained momentum in recent years due to marketability of materials that can use processed asphalt shingles. The role of recycled roofing shingle as an ingredient in hot mix asphalt pavements has been considered as well [2, 3].

This article describes a new sustainable re-roofing technology utilizing amorphous silicon photovoltaic (PV) laminates integrated with metal roof panels, dense fiberglass

insulation and phase change material (PCM) heat sink. The installation was performed during September-October, 2009 by a research team with members from Metal Construction Association (MCA), CertainTeed Corp., Uni-Solar, Phase Change Energy Solutions and Oak Ridge National Laboratory (ORNL). MCA is a North American trade association of metal building manufacturers, builders, and material suppliers; CertainTeed is a manufacturer of thermal insulation and building envelope materials; Uni-Solar produced the amorphous silicon photovoltaic (PV) laminates used in the test roof; and Phase Change Energy manufactured the PCM.

The test roof was installed on an attic in the Envelope Systems Research Apparatus (ESRA) facility on the ORNL campus. This experimental roof is designed for installation directly on top of existing shingles, precluding the need for recycling or disposal to landfills. Field test data are presented from the experimental attic and a traditional shingle-roof attic that was used as a control attic to compare and evaluate the re-roofing technology. Both tested attics incorporated ridge and soffit vents. Further details of the attic assemblies are provided by Kosny et al. [4] and Miller et al. [5].

Experimental Roof Description

Figure 1 shows the attic roofs located on the ESRA facility. On the PV-PCM roof, three metal panels with pre-installed PV laminates are visible; they're labelled from left-to-right as panels 5, 6 and 7, as shown in the figure.

Figure 1. Shingle roof and photo-voltaic (PV) - phase change material (PCM) roof attics

The PV-PCM roof consisted of a layer of macro-encapsulated bio-based PCM placed on an oriented strand board (OSB) roof deck, followed by a 2-cm thick layer of dense fiberglass insulation with a reflective surface facing the sky, and metal panels with pre-installed PV laminates on top [4]. The metal panels were placed on top of metal sub-purlins that provided an air gap of about 50.8 mm (2 inches) over the fiberglass insulation; the air gap is vented both at the ridge and the eave. The PCM had nominal melting and freezing temperatures of 29.01°C (84.2°F) and 23.26°C (73.8°F), and a latent heat of 210 Joules/gram (J/g). The threshold temperatures to initiate melting and freezing were 26.3°C (79.3°F) and 24.2°C (75.6°F), respectively. The PCM was macro-packaged between two layers of heavy-duty plastic foil forming arrays of PCM cells. The fibreglass insulation had a thermal resistance of 0.76 $m^2 \cdot K/W$ (4.3 $ft^2 \cdot hr. \cdot °F/Btu$). Air cavities between PCM cells and air gap above the fiberglass insulation provided above-sheathing ventilation to help reduce the attic-generated cooling loads during summer.

The PV laminates are PVL-144 models from Uni-Solar. Each laminate contains 22 triple junction amorphous silicon solar cells connected in series. The silicon cells had

dimensions of 356 mm by 239 mm (14 inches by 9.4 inches). The rated maximum power of these laminates is 144 Watts (W), with corresponding operating voltage and current of 33 Volts (V) and 4.36 Amperes (A), respectively. In PV laminates, sunlight is converted into both electricity and heat [6]. In case of building integrated applications, the relatively high solar absorption of amorphous silicon laminates can be utilized during winter for solar heating purposes with PCM providing the necessary heat storage capacity. Conversely, PV laminates can generate increased cooling loads during summer. In this case, the PCM heat sink is expected to offset the effect of PV laminates and reduce summer cooling loads.

Data Acquisition Systems

Heat flux transducers and type T copper-constantan thermocouples were placed in all ESRA test attics to measure the heat flows and temperatures. Thermocouples were located at various places within the roof, inside the attic and within the attic floor deck. Heat flux transducers (HFT) were located at the roof and the attic floor deck in each attic. An on-site weather station recorded incident solar flux, long wave radiation beyond 3 micrometers (μm), ambient dry bulb temperature, ambient air relative humidity, etc.

PV generated voltages and currents were monitored using a Campbell Scientific datalogger. Current was measured using precision shunt resistors that converted the current into millivolt signals that were recorded by the datalogger. Since the PV voltages exceeded the maximum allowable 5 V input into the datalogger, voltage dividers were incorporated to reduce the voltage input to acceptable levels. Here, the selected voltage dividers used a 10:1 ratio, yielding an approximate 4.8 V input for the

maximum 48 V output of the laminates. PV laminates 5 and 7 were loaded at the "MPP", or Maximum Power Point, using fixed 8.2 ohm (±1 percent) non-inductive resistors with 1200 W power dissipation capacity. With laminate 6, an electronic load incorporating a metal–oxide–semiconductor field-effect transistor (MOSFET) was used, which allowed the voltage to be set at a fixed value; 22 V direct current (DC) for this test. When the PV output reached the predetermined set point, the voltage was locked and the current continued to rise to the maximum PV output. As the solar intensity faded, the current decreased until the set point was reached, beyond which both the voltage and current decreased to zero.

Further, to assess the performance of the PV laminates, the incident solar energy was detected using an on-site Precision Spectral Pyranometer (PSP). The PSP measured the global irradiance on a surface with the same slope as the attic roofs. It is from Eppley Laboratory and measured the total incident solar heat flux over the spectral range of 0.285 - 2.8 µm, which contains more than 95 percent of the solar energy [7]

Results and Discussion

In the following sections, data from the test attics, PV laminates and the weather station are presented and discussed. Here, data collected from winter 2009 to summer 2010 are shown. Specifically, the collection period extended from November 13, 2009 to September 10, 2010.

Attic Performance Data

Figure 2 shows 24-hour variations of attic roof surface temperatures and outside

ambient temperatures over typical winter and summer days, January 9, 2010 and July 15, 2010. Usually, no significant temperature differences are seen between the two roofs. However, during the winter night, the PV-PCM roof shows slightly lower temperatures than the shingle roof, indicating lower heat losses to the night sky. The PV laminates and shingle roof had infrared emissivities of 0.67 and 0.91, respectively, which influence the night-time radiation heat losses. Lower temperature of the PV-PCM roof surface is due to the differences in optical properties and the overall design of the roofs. The roof temperature maxima of both attics were significantly higher than the ambient temperatures during the day-time hours. During nights, the roof temperatures were similar to, or slightly below, ambient.

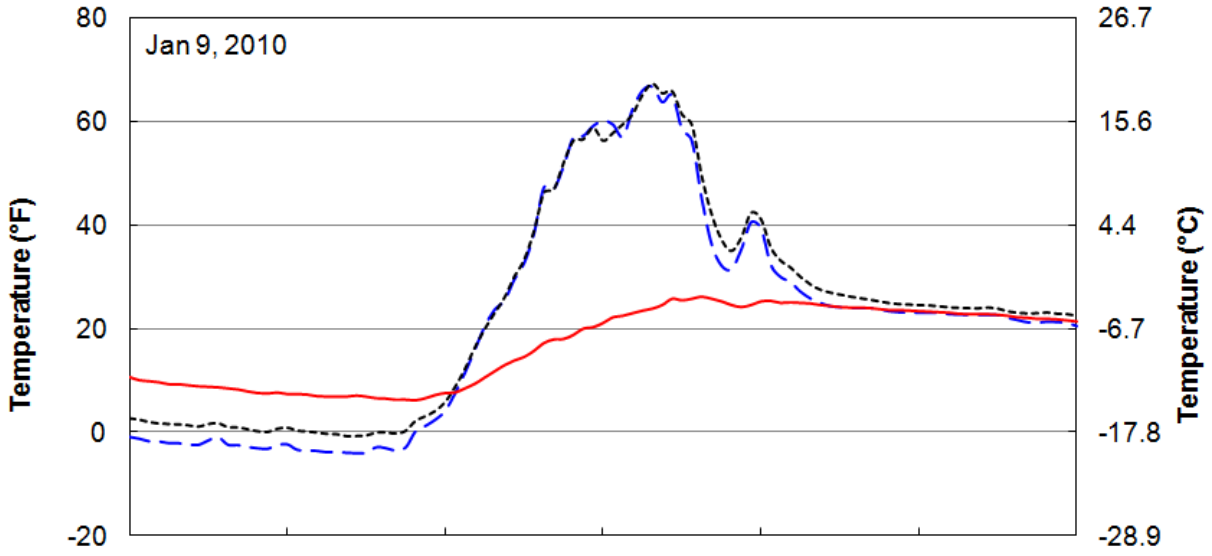

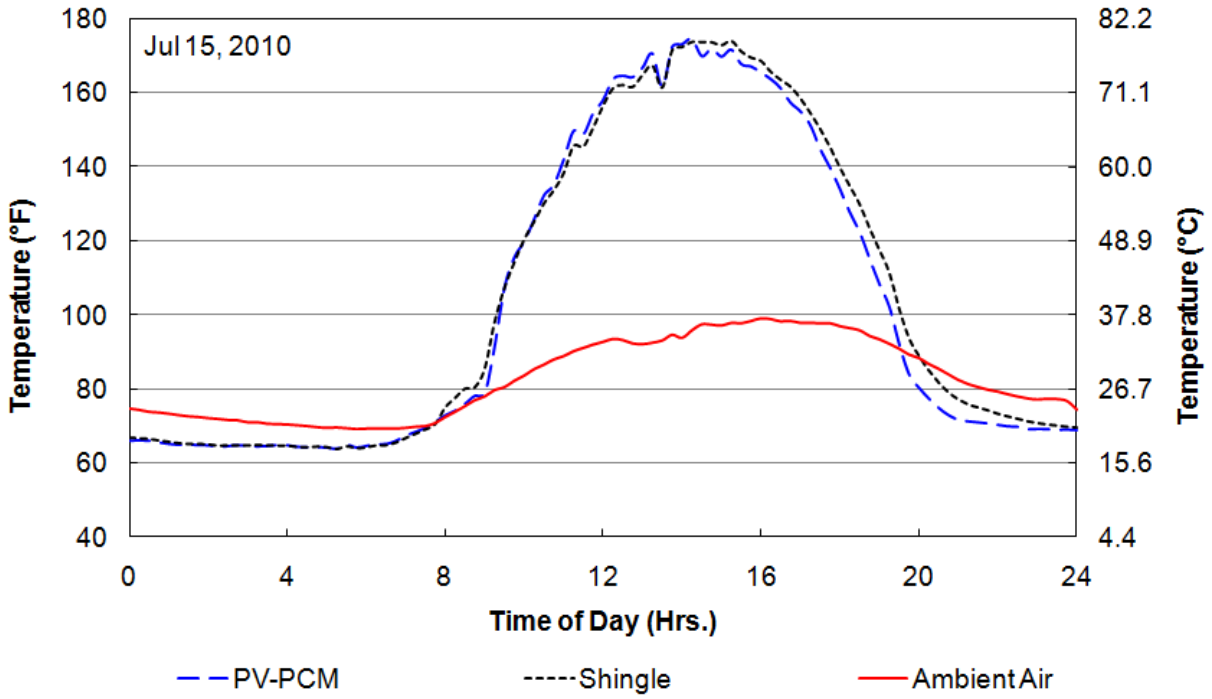

Figure 2. Daily roof surface temperature variations

Since the attic experiences large temperature fluctuations, the roof system is an attractive candidate for the application of PCM to reduce those fluctuations and, hence, the attic-generated thermal loads on the conditioned space. To evaluate the influence of the PCM on the attic behavior, temperatures above and below the PCM layer were recorded. Figure 3 shows the variation of the weekly maximum and minimum PCM layer temperatures. Also shown for comparison are the threshold temperatures at which phase changes - melting and freezing - are initiated. The weekly maximum temperatures indicate that, for several weeks during the winter (November 20, 2009 to February 11, 2010), the PCM did not melt. Conversely, the weekly minima indicate that during peak summer (June 11, 2010 to August 27, 2010), the PCM was always in molten form. These periods are indicated by “No PCM Cycling” in the figure, when the PCM did

not undergo a full charging-discharging cycle.

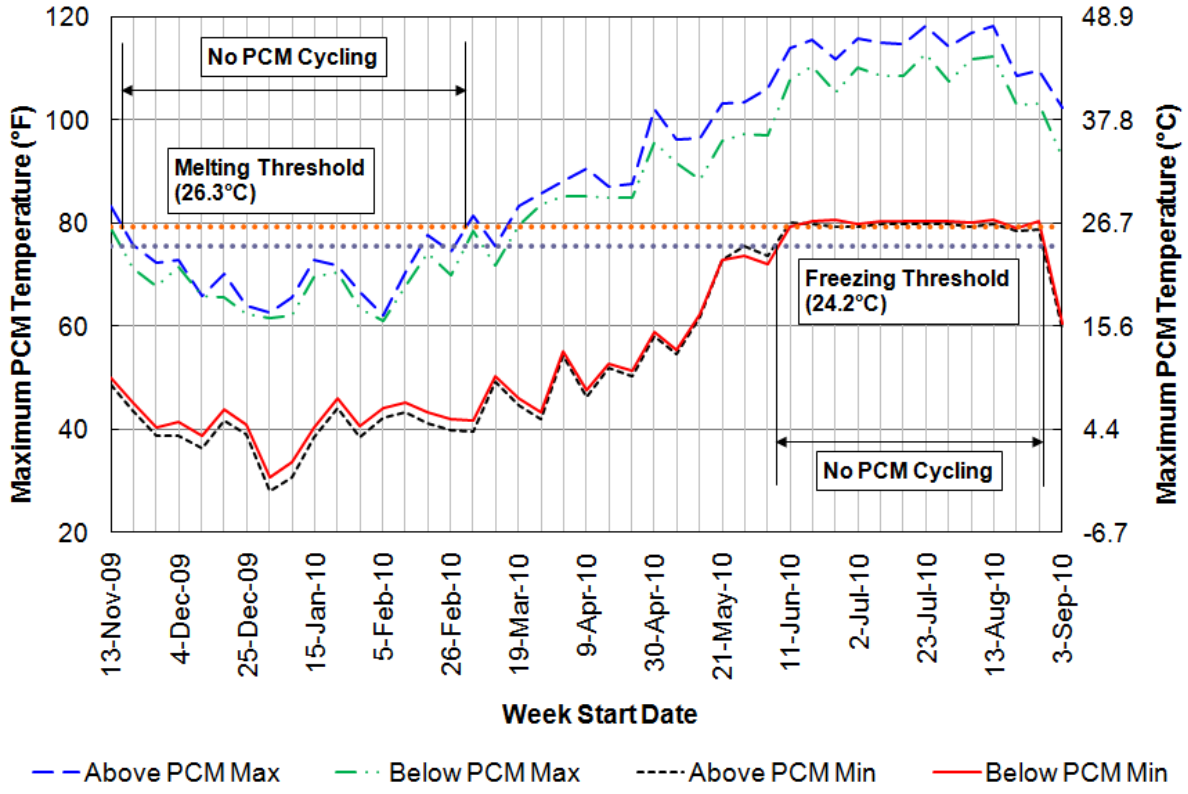

Figure 3. Weekly maximum and minimum PCM surface temperatures

Figure 4 shows the attic center temperature variations during two typical winter and summer days. The effectiveness of the PV-PCM roof in damping the attic temperature fluctuations, and hence, reducing the load on the conditioned space, is apparent from the temperature distributions. Based on data presented in Figure 3, during both January 9 and July 15, the PCM was either fully frozen or fully melted and did not undergo any phase change. Hence, the damped temperature fluctuations are a result of the roof insulation and above-sheathing ventilation.

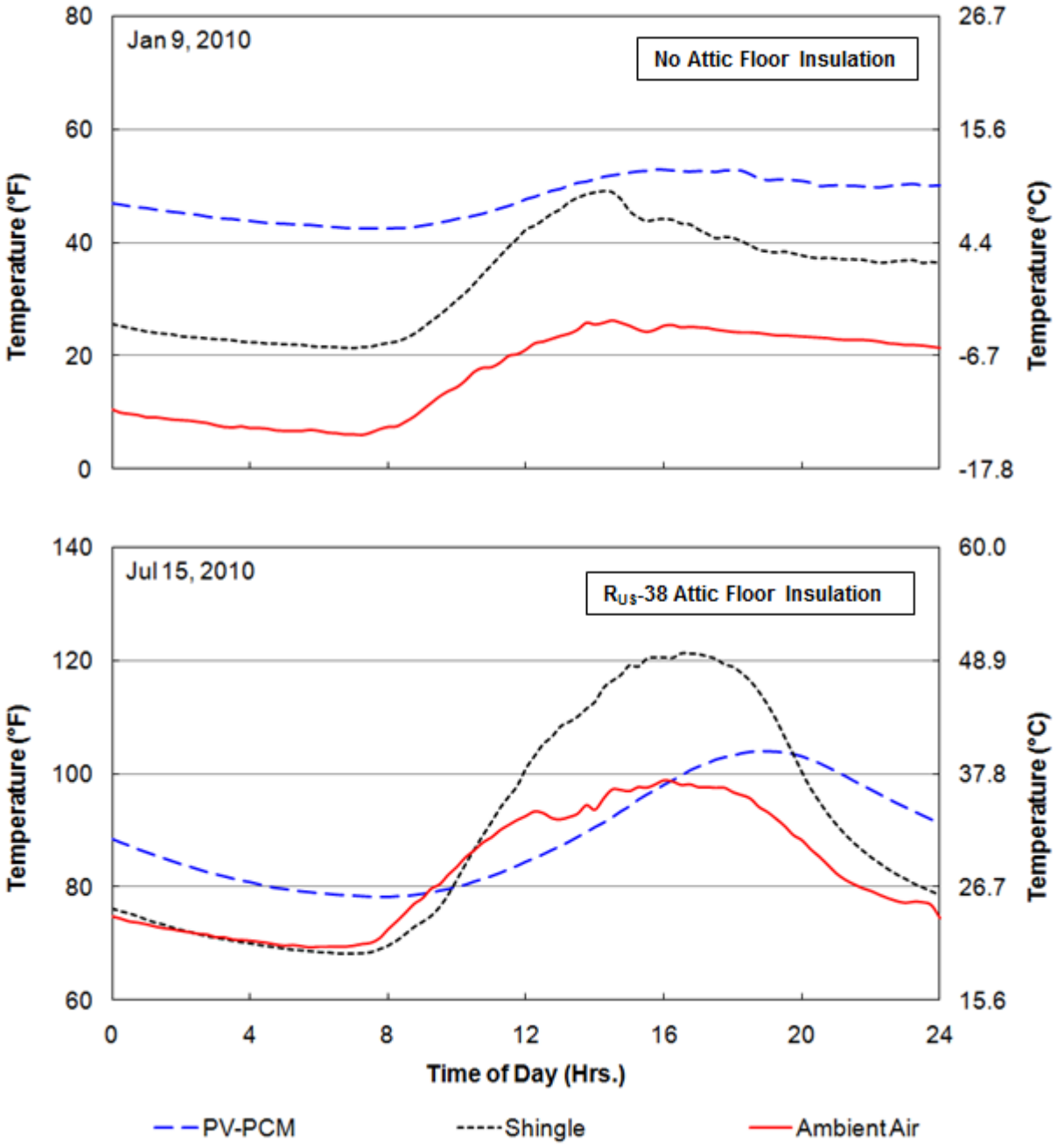

Figure 4. Daily attic center temperature variations

Also evident is a peak load shift by about 2 hours in the temperature histories from July 15. On March 9, 2010, 12 inch thick fiberglass batts of 6.7 m^2·K/W (38 ft^2·hr.·°F/Btu) thermal resistance were added to the attic floors. This potentially affected the attic

center temperatures due to reduced heat transfer between the attic and the conditioned space below. There was no attic floor insulation before March 9.

The evaluation period has been divided into the winter-spring and spring-summer periods, since the PV-PCM roof behavior is expected to be different due to the different weather conditions. Figure 5 illustrates the weekly average attic center temperatures during the period defined as winter-spring, between November 13, 2009 and March 11, 2010. The week starting on March 12 is deemed an appropriate partition date because of the addition of attic floor insulation on March 9. On average, the PV-PCM attic remained warmer than the shingle attic by 8.3°F (4.6°C), as seen in the column chart.

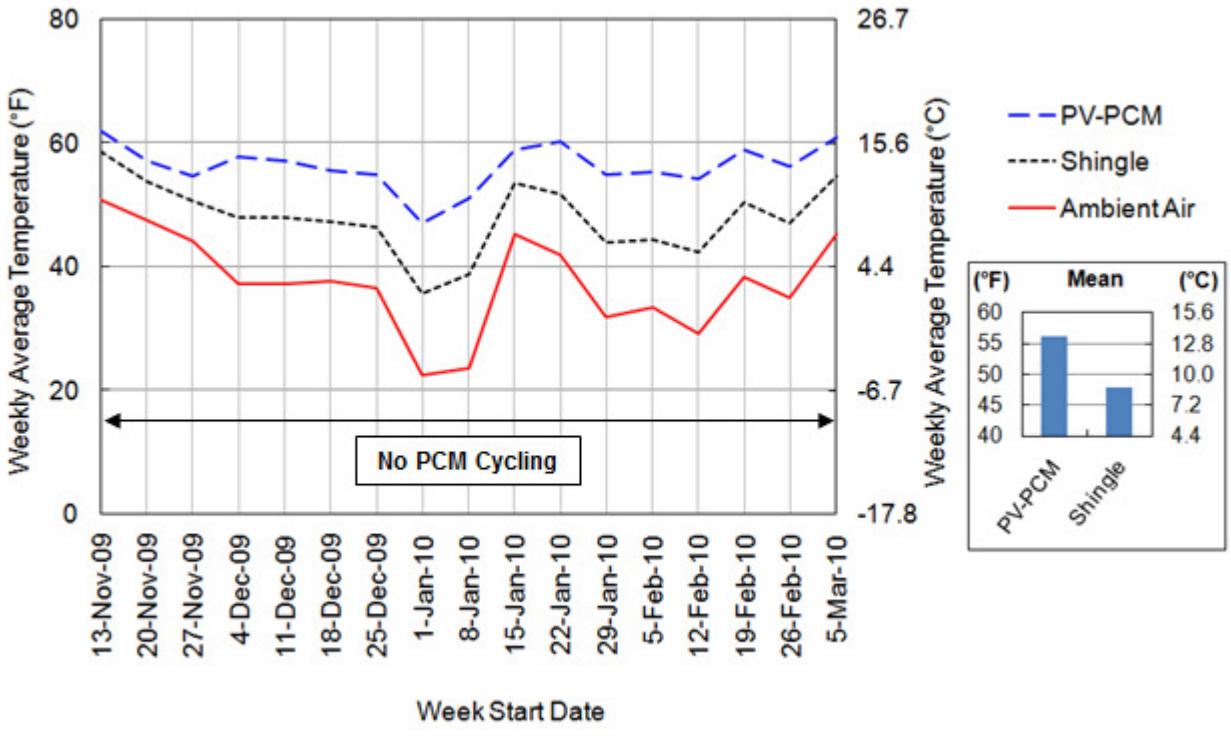

Figure 5. Average weekly attic center temperatures during winter-spring period with no attic floor insulation

Figure 6 shows the weekly minimum attic center temperatures during winter-spring, to illustrate the impact of the PV-PCM roof on the peak heating load requirements. During this time, the weekly minimum PCM attic center temperature was higher than the shingle attic by 16.1°F (8.9°C). It should be noted that during almost the entire period, the PCM was frozen and did not undergo phase change.

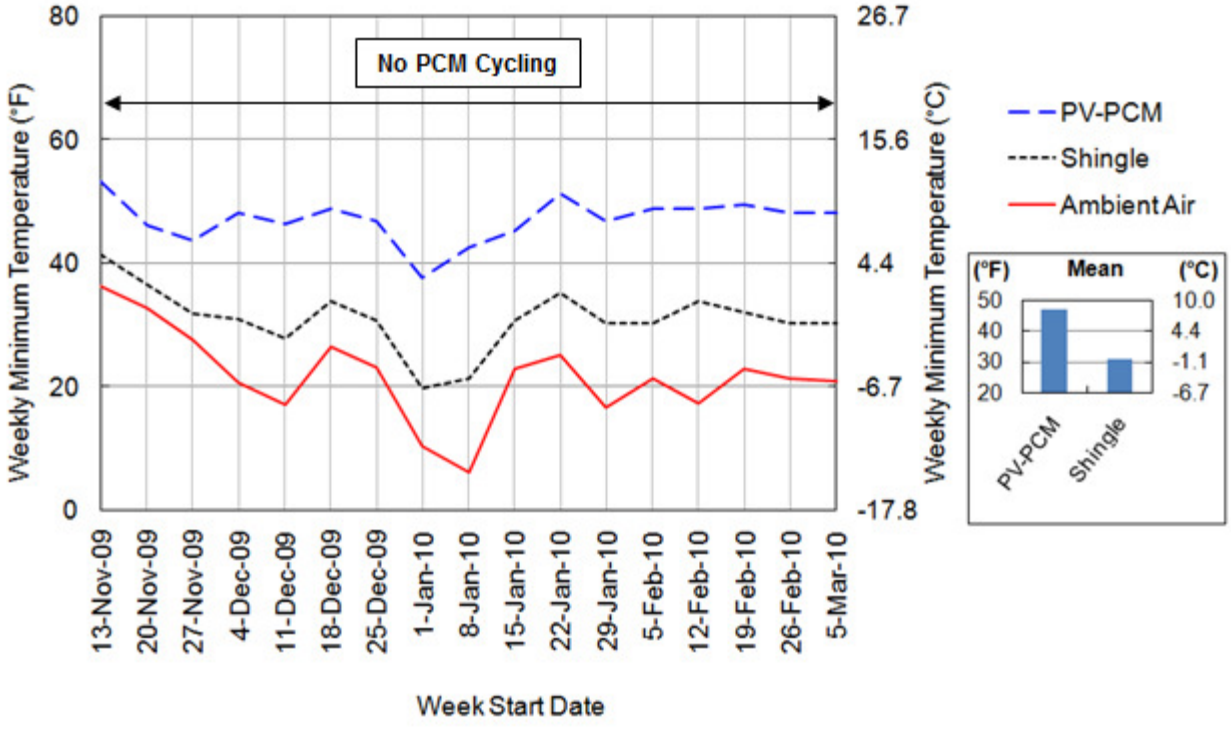

Figure 6. Minimum weekly attic center temperatures during winter-spring period with no attic floor insulation

Figure 7 shows the average weekly attic center temperatures during the spring-summer period, from March12 to September 10, 2010. During the early part of this period, with cooler outside temperatures, the temperature of the PV-PCM attic was actually higher than the shingle attic. As the weather got warmer, both attics exhibited almost identical weekly average attic temperatures.

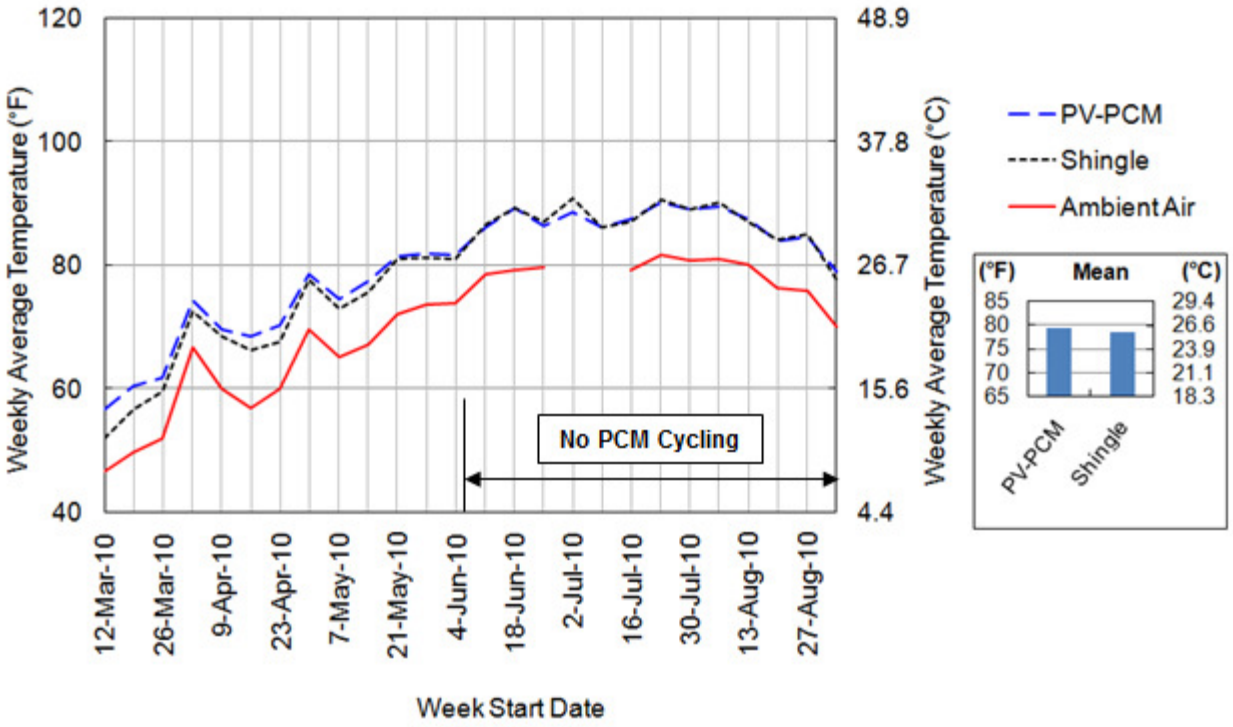

Figure 7. Average weekly attic center temperatures during spring-summer period with R_{US}-38 attic floor insulation

During summer, the peak cooling loads occurred during late-afternoons and can be related to the maximum attic temperatures, shown in Figure 8. Significant differences in maximum PV-PCM and shingle attic temperatures were observed. The weekly maximum of the PV-PCM attic center temperature was lower than the shingle attic by an average of 18.6°F (10.3°C). It should again be noted that the PCM underwent phase change cycles only during the early part of the spring-summer period, until about June 4.

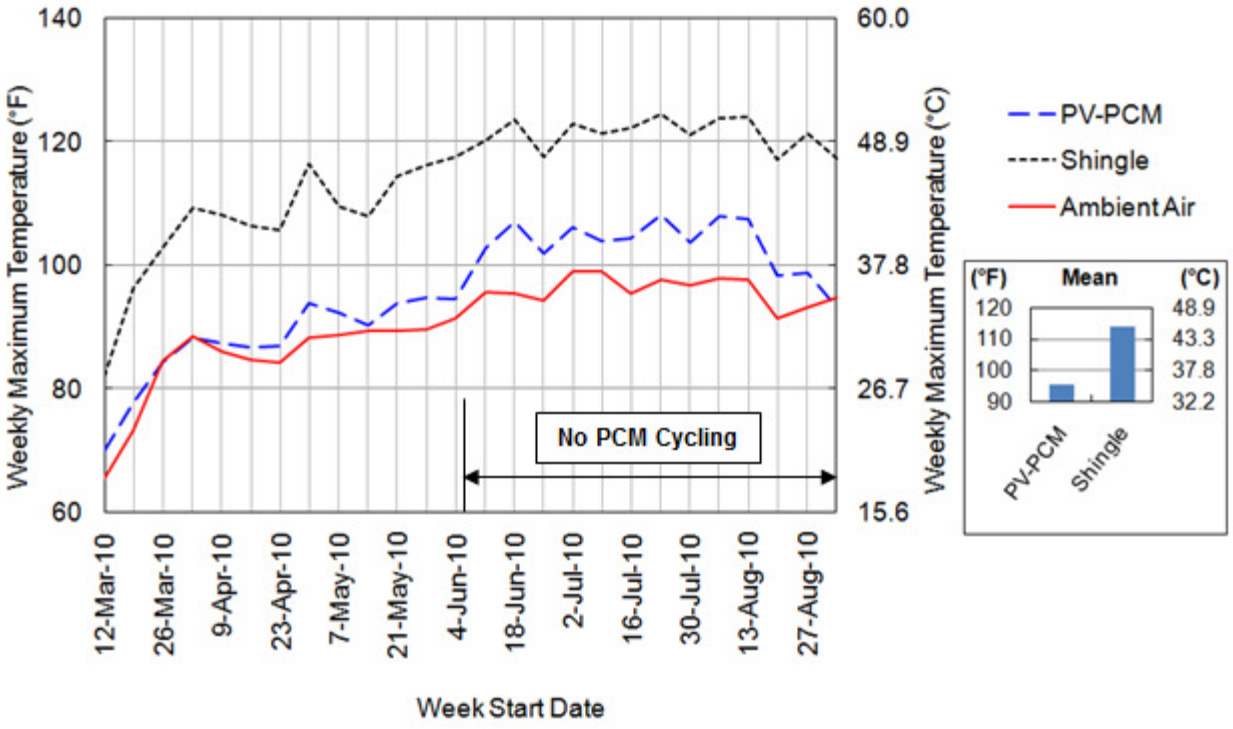

Figure 8. Maximum weekly attic center temperatures during spring-summer period with R_{US}-38 attic floor insulation

Figure 9 shows the daily heat flux variation between the attics and the conditioned space below. The sign convention for the heat transfer direction is such that the heat flow from the attics to the conditioned space is positive. Thus, positive values represent attic-generated cooling loads (heat gain by conditioned space) and negative values represent heating loads (heat loss from conditioned space). The effect of reduced attic temperature fluctuations and peak load shift due to the PV-PCM roof is seen in the heat flux distributions as well. On average, there was about a two-hour peak load shift in the PV-PCM attic. The addition of fiberglass attic floor insulation on March 9 significantly reduced the heat transfer between the conditioned space and the attics, which is evident in the heat flux histories of July 15.

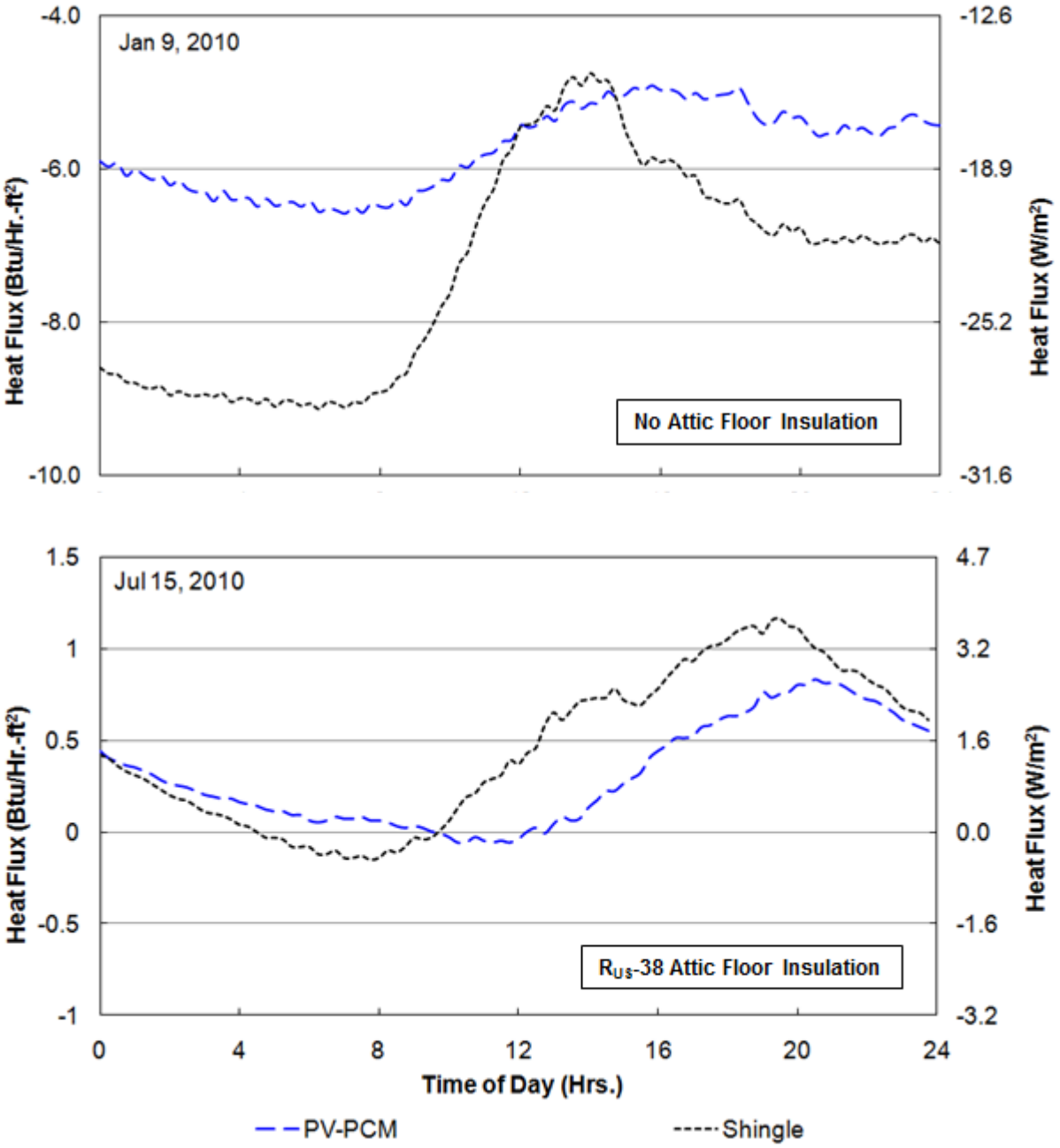

Figure 9. Daily heat fluxes between attic and conditioned space

Figure 10 shows the average weekly attic-generated cooling and heating loads, between November 13, 2009 and March 11, 2010. During winter, the shingle attic added some heat to the conditioned space, presumably during the day-time. The PV-

PCM attic essentially eliminated any heat addition to the conditioned space, and hence the cooling load, during winters. The weekly average cooling loads were 0.05 W/m^2 (0.02 Btu/hr·ft^2) and 1.14 W/m^2 (0.36 Btu/hr·ft^2) for the PV-PCM and the shingle attics, respectively.

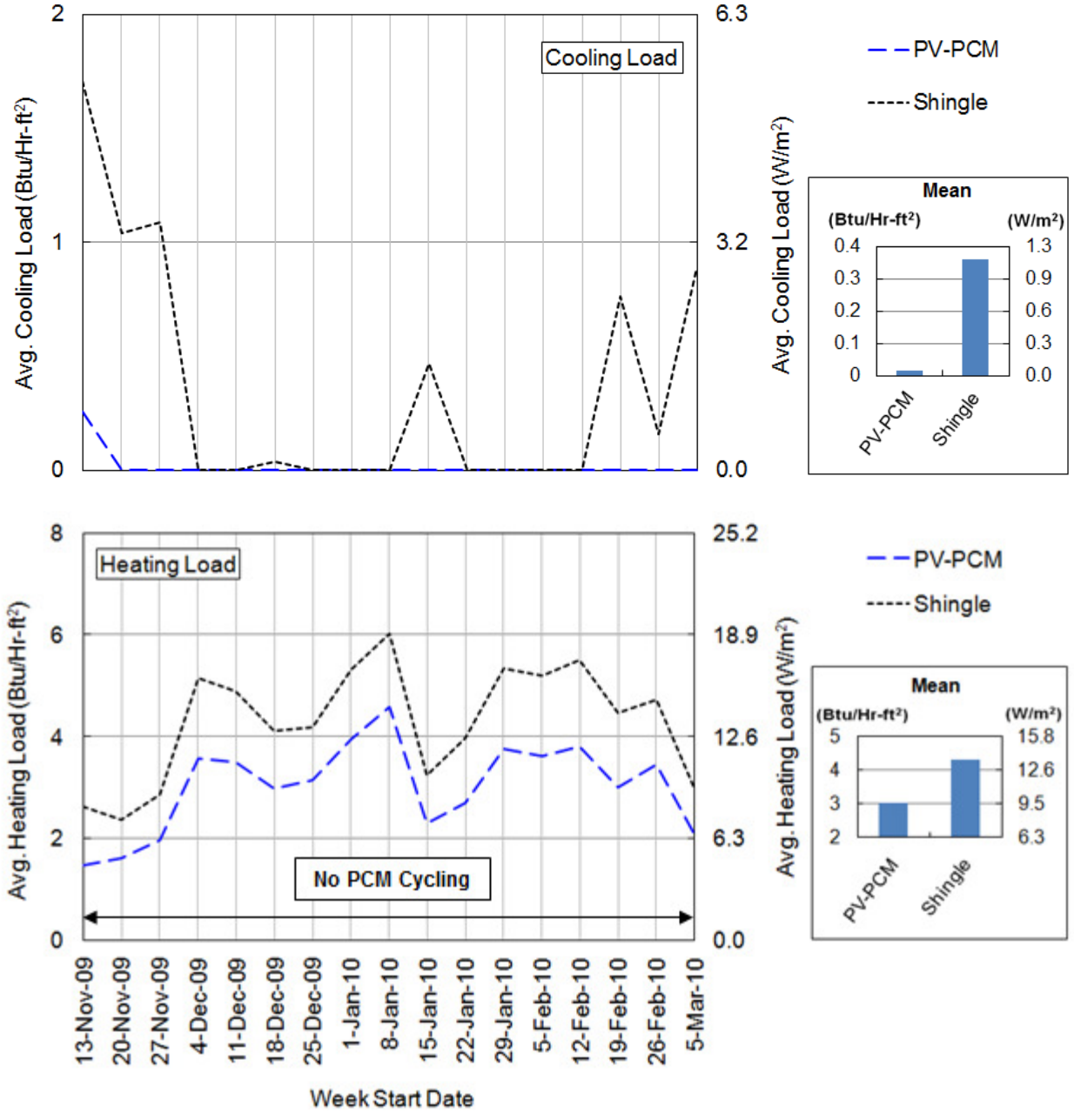

Figure 10. Average weekly attic-generated loads during winter-spring period (with no attic floor insulation)

The attic-generated heating loads were much more significant during this period. The PV-PCM and shingle attics generated heating loads of 9.55 W/m^2 (3.03 Btu/hr·ft^2) and 13.54 W/m^2 (4.29 Btu/hr·ft^2), respectively. The PV-PCM attic performed significantly better than the shingle attic by reducing the heating load by 30 percent.

Figure 11 shows the weekly average heat flux between March12 and September 10, 2010. As expected, the attic-generated cooling loads increased during this period and the heating loads decreased. The average cooling loads during this period were 0.74 W/m^2 (0.24 Btu/hr·ft^2) and 1.24 W/m^2 (0.39 Btu/hr·ft^2) for the PV-PCM and shingle attics; the corresponding heating loads were 0.50 W/m^2 (0.16 Btu/hr·ft^2) and 0.87 W/m^2 (0.28 Btu/hr·ft^2). During this period, both heating and cooling loads from the PV-PCM attic were more than 40 percent lower than the shingle attic. Also illustrated in the two figures are the periods during which the PCM did not undergo any phase change cycling. It should be noted that only the heat flux magnitudes are shown in Figure 10 and Figure 11. Therefore, both heating and cooling loads are positive.

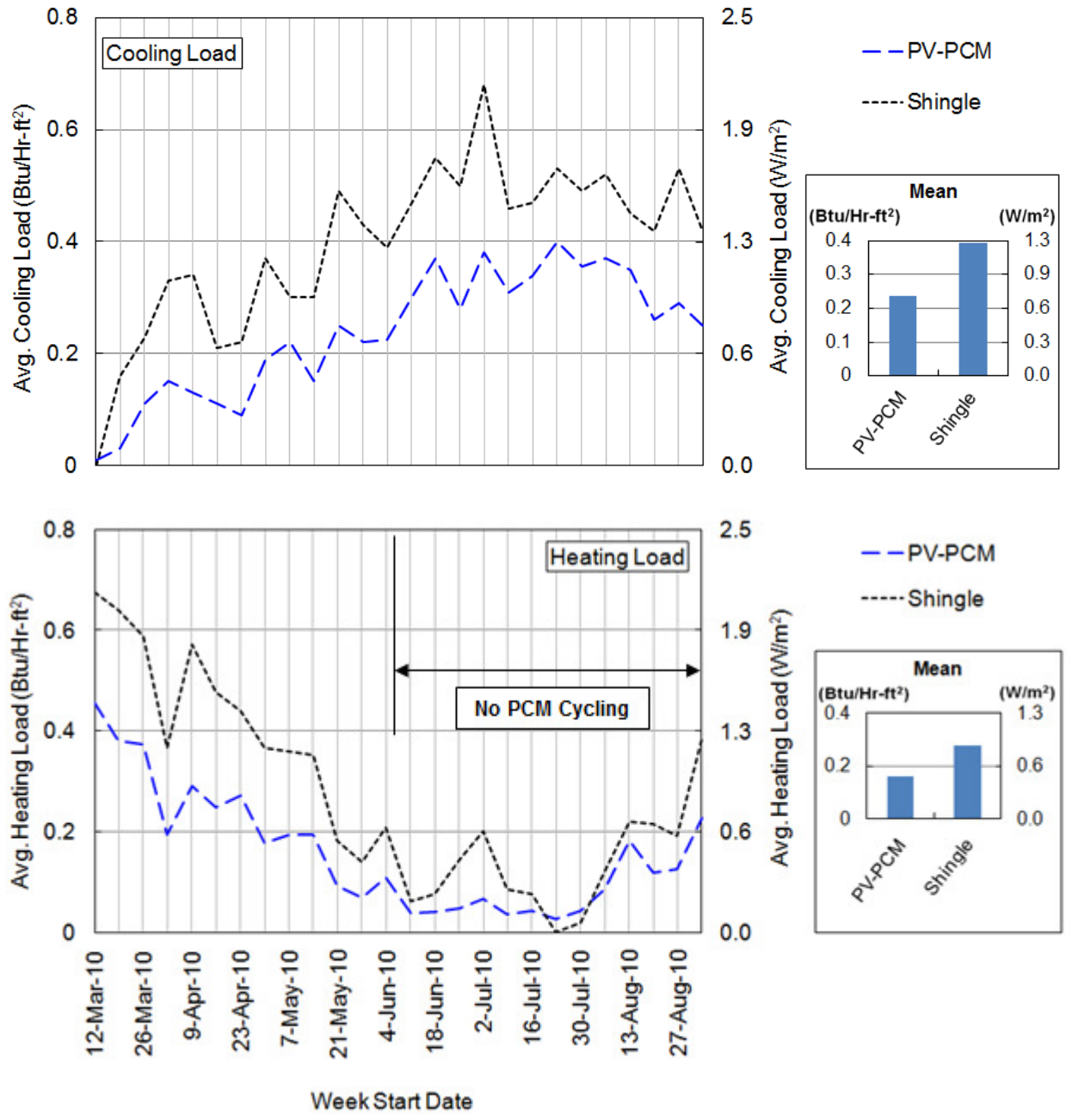

Figure 11. Average weekly attic-generated loads during spring-summer period (with R_{US}-38 attic floor insulation)

As mentioned in the above discussions, temperature data indicated that for a major portion of the evaluation period, the PCM was either fully frozen or molten with no

phase change occurring. Therefore, the damped temperature fluctuations, heating and cooling load reductions, and peak load shifts are combined effects of all roof components, which include the PV laminates, fibreglass insulation with reflective surface, PCM and the air cavities. Further, the choice of the PCM is not ideal for the weather conditions encountered and greater energy savings can be expected by using PCMs with more appropriate phase change temperatures.

For the next phase of this project, another experimental roof has been installed. This roof is identical to the current PV-PCM roof in all respects, except it does not contain any PCM. Plastic strips have been used to maintain the geometry and the air cavities for above sheathing ventilation. It is expected that comparison of the existing and new experimental roofs will enable evaluation of the PCM's influence in regulating the attic-generated heating and cooling loads.

Solar Power Generation

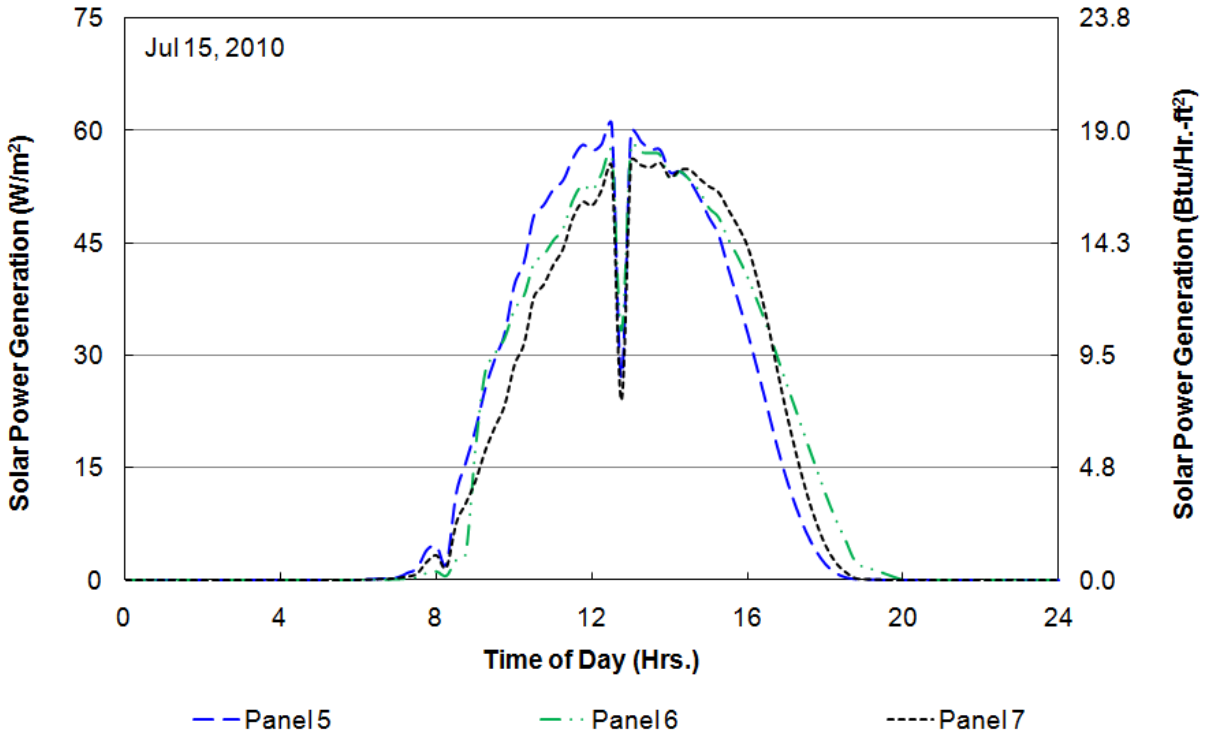

Figure 12. Daily solar power generation per unit PV collection area

This section presents the solar power generation data from the photovoltaic (PV) laminates installed on top of the PCM attic. Figure 12 shows the daily power generation from panels 5, 6 and 7, divided by the collection area of the PV laminates. All laminates have identical collection areas of 1.87 m^2 (20.13 ft^2). The power (P) is calculated using the measured voltage (V) and current (I) as:

$$P = V \times I \qquad (1)$$

The power generation follows the evolution of the solar flux incident on the panels. The peak incident solar flux was about 860 W/m^2 (~ 273 Btu/hr-ft^2) on July 15.

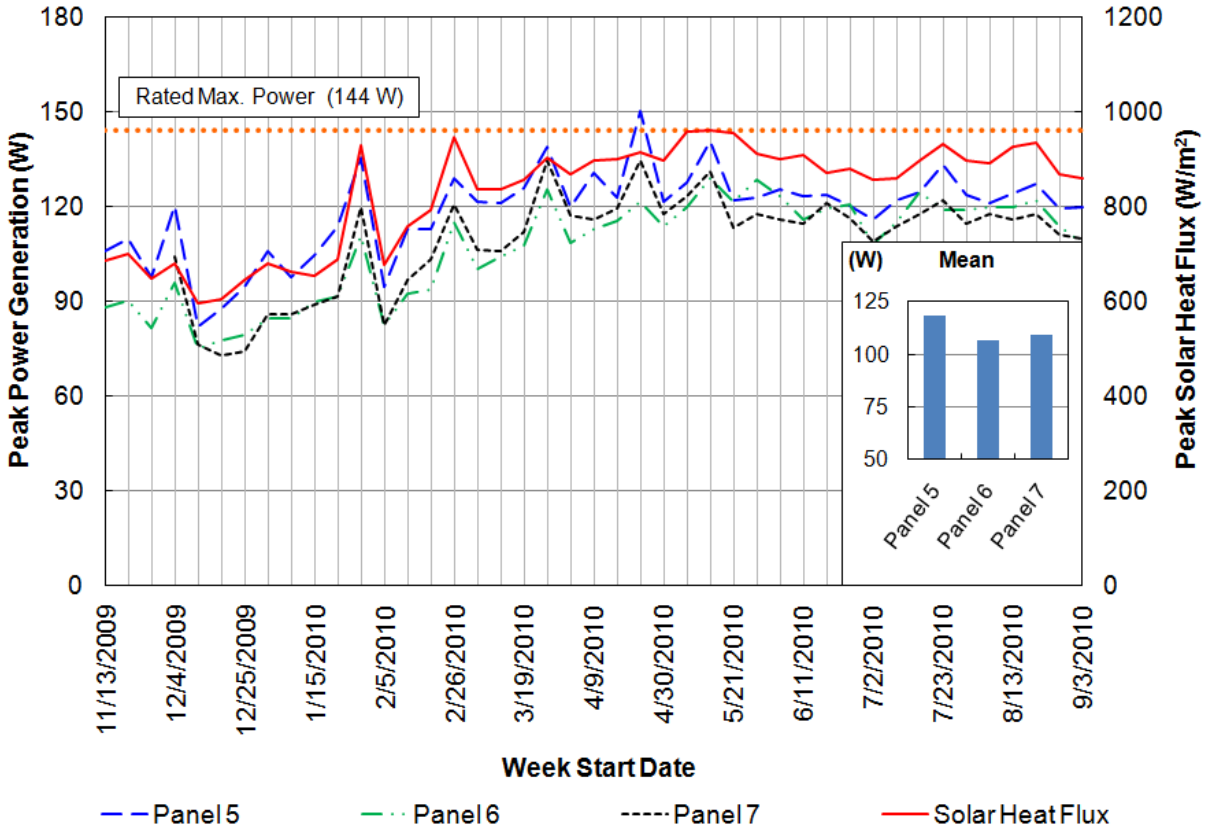

Figure 13. Weekly peak power generation by the photovoltaic laminates

Figure 13 shows the weekly peaks in the power generation and incident solar heat flux. The PV power generation is shown on the left vertical axis and the solar heat flux is on the right vertical axis. Panel 5 exhibited higher peaks than panels 6 and 7. Averaged over the collection period, the mean weekly peaks of panels 5, 6 and 7 are 118.4 W, 106.7 W and 109.2 W. Considering panel 5 as the base case (100 percent), panels 6 and 7 had 90 percent and 92 percent peak power production, respectively.

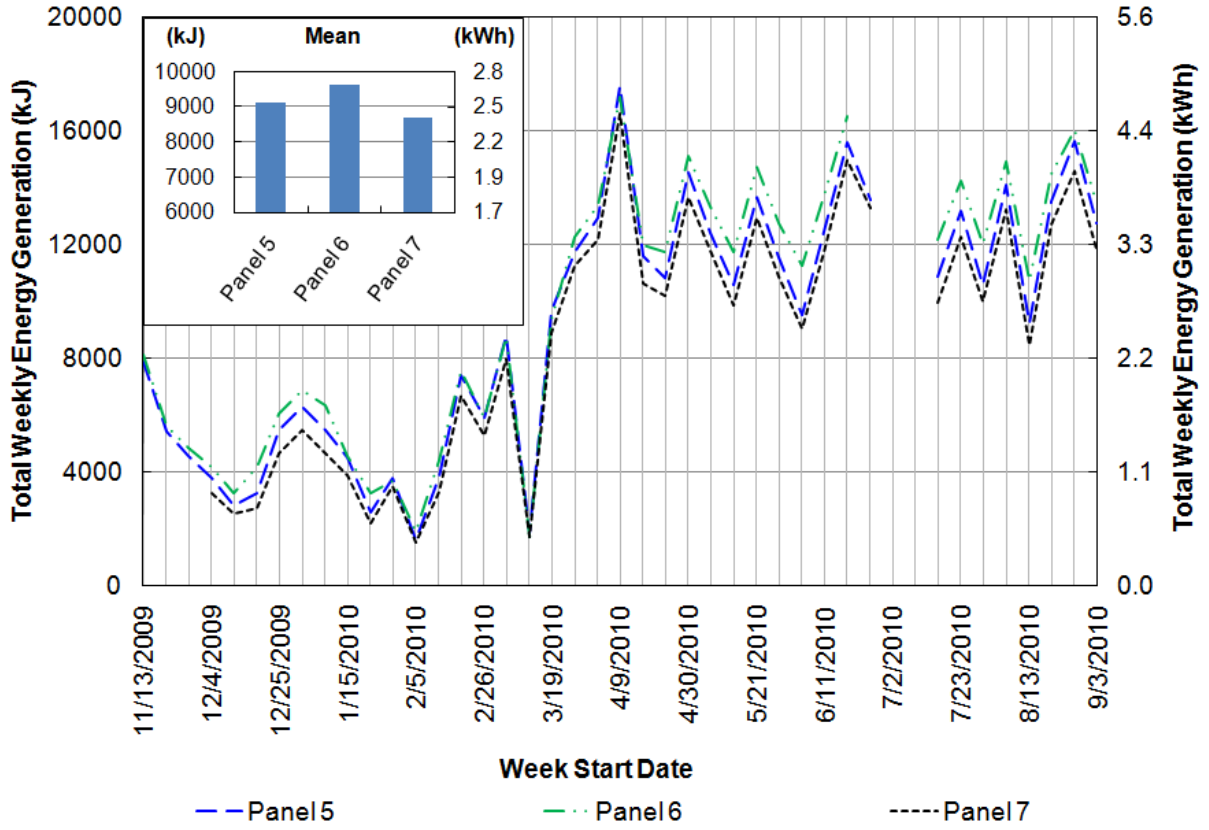

Figure 14. Weekly total energy generation by the photovoltaic laminates

Finally, the weekly total electrical energy generation was calculated and is shown in Figure 14. Energy generation is calculated through numerical integration of the power generation over the collection time. Only partial data were available during some weeks in June and July 2010; therefore, the weekly energy generation could not be calculated. The mean weekly generation was 9111.4 kJ, 9613.4 kJ and 8696.2 kJ for panels 5, 6 and 7, respectively. With respect to panel 5 (100 percent), panels 6 and 7 had 105 percent and 95 percent energy production, respectively. Therefore, based on available data, PV panels with fixed loads yield higher power peaks, while dynamically-loaded panels generate more energy over the collection period.

Some differences were consistently observed in the power generation from panels 5 and 7. Since the circuits connected to both panels contain the same fixed load, 8.2 ohms, they can be expected to generate similar power, within experimental uncertainties. Whether these differences are purely the results of such uncertainties, or are caused by systemic differences in their setup, needs to be further evaluated.

Summary and Conclusions

During fall 2009, an experimental attic using a roof retrofit technology was installed at the ORNL Envelope Systems Research Apparatus facility, and compared to a control attic with a shingle roof. Field-test data collected between November 13, 2009 and September 10, 2010 are presented in this report. The experimental roof can be installed directly over existing roofs without requiring removal of the old materials. It consists of roof-integrated PV laminates, dense fiberglass insulation with reflective foil facing and PCM heat sink.

The test data demonstrated that this retrofit technology can be very effective in improving energy performance of existing roofs. During winter, the PV-PCM attic showed a 30 percent reduction in the heating load compared to a conventional shingle attic. Conversely, during spring and summer, the attic generated cooling load from the PV-PCM attic was 40 percent lower than the shingle attic. It is noted that the PCM did not undergo a full “charging-discharging” cycle for a number of weeks during peak winter and peak summer. The current configuration and choice of phase change temperatures resulted in the PCM not being a major contributor towards energy savings. However, roof and attic systems are attractive candidates for the application of

PCM due to the large temperature fluctuations experienced by the attic, as demonstrated by the shingle attic data. Using a PCM, or combination of PCMs with different phase change temperatures, better tuned to the climate and optimizing the placement of the PCM can yield higher energy savings.

Further, the PV-PCM roof generates solar electricity that can be fed back to the supply grid. The electricity generation coupled with the peak load shifting in the PV-PCM attic can offset the peak demands on the power plants and lower costs for the consumer due to greater usage of off-peak power. Three (3) PVL-144 model amorphous silicon PV laminates were evaluated. Two PV panels had fixed load resistors and the third contained a dynamic load to lock the voltage at a certain value while the current increased to the maximum PV output. Test data indicate that dynamically-loaded PV panels generate more energy over the collection periods, while the fixed load panels yield higher power peaks.

Acknowledgements

The authors would like to thank Joe Harter (ATAS), Mike Walters and Eric Akkashian (UniSolar), Sam Yuan (CertainTeed) and Pete Horvath (Phase Change Energy) for their contributions. The technical assistance of Ed Reed in setting up the data acquisition systems is gratefully acknowledged.

References

1. Townsend, T.; Powell, J.; Chad, X.; 2007. “Environmental Issues Associated with Asphalt Shingle Recycling,” Report prepared for Construction Materials Recycling

Association Asphalt Shingle Recycling Project, US EPA Innovations Workgroup by Innovative Waste Consulting Services, LLC Gainesville, Florida - October 19, 2007.

2. Sengoz, B.; Topal, A.; 2005. "Use of Asphalt Roofing Shingle Waste in HMA," *Construction and Building Materials*, v 19, n 5, p 337-346.
3. Decker, D. S.; 2002. "The Road to Shingle Recycling," *Recycling Today*, v 40, n 9, 28-32.
4. Kosny J., Biswas K., Miller W., Childs P., and Kriner S. "Sustainable Retrofit of Residential Roofs Using Metal Roofing Panels, Thin-Film Photovoltaic Laminates and PCM Heat Sink Technology," *Journal of Building Enclosure Design*, National Institute of Building Sciences, Building Enclosure Technology and Environment Council (BETEC), Winter 2011/3.
5. Miller, W. A., P. Wilson, and A. Karagiozis. 2006. "The Impact of Above-Sheathing Ventilation on the Thermal and Moisture Performance of Steep-Slope Residential Roofs and Attics." 15th Symposium on Hot and Humid Climates, Orlando, Fla., July.
6. van Helden, W. G. J.; van Zolingen, R. J. Ch.; Zondag, H. A.; 2004. "PV Thermal Systems: PV Panels Supplying Renewable Electricity and Heat", *Progress in Photovoltaics: Research and Applications*, v 12, n 6, 415-26.
7. ASTM G159 – 98, Standard Tables for References Solar Spectral Irradiance at Air Mass 1.5: Direct Normal and Hemispherical for a 37° Tilted Surface.